Genome-wide meta-analyses of multiancestry cohorts identify multiple new susceptibility loci for refractive error and myopia

Published in final edited form as:
Nat Genet. 2013 March ; 45(3): 314–318. doi:10.1038/ng.2554.

Genome-wide meta-analyses of multi-ethnic cohorts identify multiple new susceptibility loci for refractive error and myopia

Virginie J.M. Verhoeven[*,1,2], **Pirro G. Hysi**[*,3], **Robert Wojciechowski**[*,4,5], **Qiao Fan**[*,6], **Jeremy A. Guggenheim**[*,7], **René Höhn**[8,*], **Stuart MacGregor**[9], **Alex W. Hewitt**[10,11], **Abhishek Nag**[3], **Ching-Yu Cheng**[6,12,13], **Ekaterina Yonova-Doing**[3], **Xin Zhou**[6], **M. Kamran Ikram**[6,12,13], **Gabriëlle H.S. Buitendijk**[1,2], **George McMahon**[14], **John P. Kemp**[14], **Beate St. Pourcain**[15], **Claire L. Simpson**[4], **Kari-Matti Mäkelä**[16], **Terho Lehtimäki**[16], **Mika Kähönen**[17], **Andrew D. Paterson**[18], **S. Mohsen Hosseini**[18], **Hoi Suen Wong**[18], **Liang Xu**[19], **Jost B. Jonas**[20], **Olavi Pärssinen**[21,22], **Juho Wedenoja**[23], **Shea Ping Yip**[24], **Daniel W. H. Ho**[7,24], **Chi Pui Pang**[25], **Li Jia Chen**[26], **Kathryn P. Burdon**[27], **Jamie E. Craig**[27], **Barbara E. K. Klein**[28], **Ronald Klein**[28], **Toomas Haller**[29], **Andres Metspalu**[29], **Chiea-Chuen Khor**[6,12,30,31], **E-Shyong Tai**[6,32,33], **Tin Aung**[12,13], **Eranga Vithana**[13], **Wan-Ting Tay**[13], **Veluchamy A. Barathi**[12,13,33], **CREAM**[34], **Peng Chen**[6], **Ruoying Li**[6], **Jiemin Liao**[12], **Yingfeng Zheng**[13], **Rick T. Ong**[6], **Angela Döring**[35,36], **DCCT/EDIC Research Group**[34], **David M. Evans**[14], **Nicholas J. Timpson**[14], **Annemieke J.M.H. Verkerk**[37], **Thomas Meitinger**[38], **Olli Raitakari**[39,40], **Felicia Hawthorne**[41], **Tim D. Spector**[3], **Lennart C. Karssen**[2], **Mario Pirastu**[42], **Federico Murgia**[42], **Wei Ang**[43], **WTCCC2**[34], **Aniket Mishra**[9], **Grant W. Montgomery**[9], **Craig E. Pennell**[43], **Phillippa M. Cumberland**[44,45], **Ioana Cotlarciuc**[46], **Paul Mitchell**[47], **Jie Jin Wang**[10,47], **Maria Schache**[48], **Sarayut Janmahasathian**[49], **Robert P. Igo Jr**[49], **Jonathan H. Lass**[49,50], **Emily Chew**[51], **Sudha K. Iyengar**[49,50,52], **the Fuchs' Genetics Multi-Center Study Group**[34], **Theo G.M.F. Gorgels**[53], **Igor Rudan**[54], **Caroline Hayward**[55], **Alan F. Wright**[55], **Ozren Polasek**[56], **Zoran Vatavuk**[57], **James F. Wilson**[54], **Brian Fleck**[58], **Tanja Zeller**[59], **Alireza Mirshahi**[8], **Christian Müller**[59], **Andre' G. Uitterlinden**[2,37], **Fernando Rivadeneira**[2,37], **Johannes R. Vingerling**[1,2], **Albert Hofman**[2], **Ben A. Oostra**[60], **Najaf Amin**[2], **Arthur A.B. Bergen**[53,61,62], **Yik-Ying Teo**[6,63], **Jugnoo S. Rahi**[44,64], **Veronique Vitart**[55], **Cathy Williams**[15], **Paul N. Baird**[10], **Tien-Yin Wong**[6,12,13], **Konrad Oexle**[38], **Norbert Pfeiffer**[8], **David A. Mackey**[10,11], **Terri L. Young**[41], **Cornelia M. van Duijn**[2], **Seang-Mei Saw**[*,6,12,13,33], **Joan E. Bailey Wilson**[*,4], **Dwight Stambolian**[*,65], **Caroline C. Klaver**[*,1,2], and **Christopher J. Hammond**[*,3]

Corresponding author Correspondence should be addressed to C.C.W.K. c.c.w.klaver@erasmusmc.nl..
*These authors contributed equally to this work.

Author contributions V.J.M.V, P.G.H., R.W., C.J.H., C.C.W.K, A.W.H., D.A.M., T.L.Y., and C.M.v.D. performed analyses and drafted the manuscript. C.C.W.K, D.S., C.J.H., J.E.B.W., S.M.S., C.M.v.D., A.H., D.A.M., S.M., A.P., V.V, C.W., P.N.B., T.Y.W., J.R., T.L.Y., K.O., O.P., S.P.Y., J.G., A.M., M.P., S.K.I., and N.P. jointly conceived the project and supervised the work. J.E.B.W., S.M.S., D.A.M., T.L.Y., C.J.H., C.C.W.K, D.S., J.E.B.W., C.M.v.D., R.W., P.G.H., V.J.M.V., K.O., Y.Y.T., T.Y.W., P.N.B., V.V., N.A., B.A.O., A.H., J.R.V., F.R., A.G.U., N.P., C.M., A.M., T.Z., B.F., J.F.W., Z.V., O.P., A.F.W., C.H., I.R., S.K.I., E.C., J.H.L., R.P.I.J., S.J., M.S., J.J.W., P.M., I.C., J.S.R., P.M.C., C.E.P., G.W.M., A.M., W.A., F.M., M.P., L.C.K., T.D.S., E.Y.D., A.N., O.R., C.C.K., T.M., A.D., R.T.O., Y.Z., J.L., R.L., P.C., V.A.B., W.T.T., E.V., T.A., E.S.T., C.C.W.K., A.M., T.H., R.K., B.E.K.K., J.E.C., K.P.B., L.J.C., C.P.P., D.W.H.H., S.P.Y., J.W., O.P., J.B.J., L.X., H.S.W., S.M.H., A.D.P., M.K., T.L., K.M.M., C.L.S., C.W., N.J.T., D.M.E., B.S.P., J.P.K., G.M., G.H.S., M.K.I., X.Z., C.Y.C., A.W.H., S.M., R.H., J.A.G., and Q.F. were responsible for study-specific data. G.H.S., Q.F., and J.A.G. were involved in the genetic risk score analysis. T.L.Y., A.A.B.B., T.G.M.F.G., and F.H. performed the data expression experiments. A.A.B.B., T.G.M.F.G., A.M., and S.M. were involved in pathway analyses. J.E.B.W., S.M.S., D.A.M., T.L.Y., K.O., T.Y.W., P.N.B., T.G.M.F.G., S.K.I., E.C., J.J.W., A.J.M.H.V., C.C.K., B.E.K.K., S.P.Y., C.W., N.J.T., G.H.S., M.K.I., A.W.H., and J.A.G. critically reviewed the manuscript.

Competing financial interests The authors declare no competing financial interests.

URLs R, http://www.r-project.org; Locuszoom, http://csg.sph.umich.edu/locuszoom; Gene Expression Omnibus, http://www.ncbi.nlm.nih.gov/geo/query/acc.cgi?acc=GSE20191; Ingenuity, http://www.ingenuity.com

[1] Department of Ophthalmology, Erasmus Medical Center, Rotterdam, The Netherlands. [2] Department of Epidemiology, Erasmus Medical Center, Rotterdam, The Netherlands. [3] Department of Twin Research and Genetic Epidemiology, King's College London School of Medicine, London, UK. [4] Inherited Disease Research Branch, National Human Genome Research Institute, National Institutes of Health, Baltimore, Maryland, USA. [5] Department of Epidemiology, Johns Hopkins Bloomberg School of Public Health, Baltimore, Maryland, USA. [6] Saw Swee Hock School of Public Health, National University Health Systems, National University of Singapore, Singapore, Singapore. [7] Centre for Myopia Research, School of Optometry, The Hong Kong Polytechnic University, Hong Kong, Hong Kong. [8] Department of Ophthalmology, University Medical Center Mainz, Mainz, Germany. [9] Queensland Institute of Medical Research, Brisbane, Australia. [10] Department of Ophthalmology, Centre for Eye Research Australia (CERA), University of Melbourne, Royal Victorian Eye and Ear Hospital, Melbourne, Australia. [11] Centre for Ophthalmology and Visual Science, Lions Eye Institute, University of Western Australia, Perth, Australia. [12] Department of Ophthalmology, National University Health Systems, National University of Singapore, Singapore. [13] Singapore Eye Research Institute, Singapore National Eye Centre, Singapore, Singapore. [14] Medical Research Council Centre for Causal Analyses in Translational Medicine, School of Social and Community Medicine, University of Bristol, Bristol, UK. [15] School of Social and Community Medicine, University of Bristol, Bristol, UK. [16] Department of Clinical Chemistry, Fimlab Laboratories, Tampere University Hospital, and School of Medicine, University of Tampere, Tampere, Finland. [17] Department of Clinical Physiology, Tampere University Hospital, and School of Medicine, University of Tampere, Tampere, Finland. [18] Program in Genetics and Genome Biology, Hospital for Sick Children and University of Toronto, Toronto, Ontario, Canada. [19] Beijing Institute of Ophthalmology, Beijing Tongren Hospital, Capital Medical University. [20] Department of Ophthalmology, Medical Faculty Mannheim, Ruprecht-Karls-University Heidelberg, Mannheim, Germany. [21] Department of Health Sciences, University of Jyväskylä, Tampere, Finland. [22] Finnish Centre for Interdisciplinary Gerontology, University of Jyväskylä, Tampere, Finland. [23] Department of Public Health, Hjelt Institute, University of Helsinki, Finland. [24] Department of Health Technology and Informatics, The Hong Kong Polytechnic University, Hong Kong, Hong Kong. [25] Department of Ophthalmology and Visual Sciences, The Chinese University of Hong Kong Hong Kong Eye Hospital, Kowloon, Hong Kong. [26] Department of Ophthalmology and Visual Sciences, The Chinese University of Hong Kong, Prince of Wales Hospital, Shatin, Hong Kong. [27] Department of Ophthalmology, Flinders University, Adelaide, Australia. [28] Department of Ophthalmology and Visual Sciences, University of Wisconsin School of Medicine and Public Health, Madison, Wisconsin, USA. [29] Estonian Genome Center, University of Tartu, Tartu, Estonia. [30] Department of Pediatrics, National University of Singapore, Singapore, Singapore. [31] Division of Human Genetics, Genome Institute of Singapore, Singapore, Singapore. [32] Department of Medicine, National University of Singapore, Singapore, Singapore. [33] DUKE-National University of Singapore Graduate Medical School, Singapore, Singapore. [34] A full list of members of these consortia can be found in the Supplementary Note. [35] Institute of Epidemiology I, Helmholtz Zentrum München, German Research Center for Environmental Health, Neuherberg, Germany. [36] Institute of Epidemiology II, Helmholtz Zentrum München, German Research Center for Environmental Health, Neuherberg, Germany. [37] Department of Internal Medicine, Erasmus Medical Center, Rotterdam, The Netherlands. [38] Institute of Human Genetics, Technical University Munich, Munich, Germany. [39] Research Centre of Applied and Preventive Medicine, University of Turku, Turku, Finland. [40] Department of Clinical Physiology and Nuclear Medicine, Turku University Hospital, Turku, Finland. [41] Department of Pediatric Ophthalmology, Duke Eye Center For Human Genetics, Durham, North Carolina, USA. [42] Institute of Population Genetics, National Research Council, Sassari, Italy. [43] School of Women's and Infants' Health, University of Western Australia, Perth, Australia. [44] Medical Research Council Centre of Epidemiology for Child Health, Institute of Child Health, University College London, London, UK. [45] Ulverscroft Vision Research Group, University

College London, London, UK. [46] Imperial College Cerebrovascular Research Unit (ICCRU), Division of Brain Sciences, Department of Medicine, Imperial College London, London, UK. [47] Department of Ophthalmology, Centre for Vision Research, Westmead Millennium Institute, University of Sydney, Sydney, Australia. [48] Ocular Genetics Unit, Centre for Eye Research Australia (CERA), University of Melbourne, Royal Victorian Eye and Ear Hospital, Melbourne, Australia. [49] Department of Epidemiology and Biostatistics, Case Western Reserve University, Cleveland, Ohio, USA. [50] Department of Ophthalmology and Visual Sciences, University Hospitals Case Medical Center, Cleveland, Ohio, USA. [51] National Eye Institute, National Institutes of Health, Bethesda, Maryland, USA. [52] Department of Genetics, Case Western Reserve University, Cleveland, Ohio, USA. [53] Department of Clinical and Molecular Ophthalmogenetics, Netherlands Institute of Neurosciences (NIN), An Institute of the Royal Netherlands Academy of Arts and Sciences (KNAW), Amsterdam, The Netherlands. [54] Centre for Population Health Sciences, University of Edinburgh, Edinburgh, UK. [55] Medical Research Council Human Genetics Unit, Institute of Genetics and Molecular Medicine, University of Edinburgh, Edinburgh, UK. [56] Faculty of Medicine, University of Split, Croatia, Split, Croatia. [57] Department of Ophthalmology, Sisters of Mercy University Hospital, Zagreb, Croatia. [58] Princess Alexandra Eye Pavilion, Edinburgh, UK. [59] Clinic for General and Interventional Cardiology, University Heart Center Hamburg, Hamburg, Germany. [60] Department of Clinical Genetics, Erasmus Medical Center, Rotterdam, The Netherlands. [61] Department of Clinical Genetics, Academic Medical Center, Amsterdam, The Netherlands. [62] Department of Ophthalmology, Academic Medical Center, Amsterdam, The Netherlands. [63] Department of Statistics and Applied Probability, National University of Singapore, Singapore, Singapore. [64] Institute of Ophthalmology, Moorfields Eye Hospital, London, UK. [65] Department of Ophthalmology, University of Pennsylvania, Philadelphia, Pennsylvania, USA.

Abstract

Refractive error is the most common eye disorder worldwide, and a prominent cause of blindness. Myopia affects over 30% of Western populations, and up to 80% of Asians. The CREAM consortium conducted genome-wide meta-analyses including 37,382 individuals from 27 studies of European ancestry, and 8,376 from 5 Asian cohorts. We identified 16 new loci for refractive error in subjects of European ancestry, of which 8 were shared with Asians. Combined analysis revealed 8 additional loci. The new loci include genes with functions in neurotransmission (*GRIA4*), ion channels (*KCNQ5*), retinoic acid metabolism (*RDH5*), extracellular matrix remodeling (*LAMA2, BMP2)*, and eye development (*SIX6, PRSS56*). We also confirmed previously reported associations with *GJD2* and *RASGRF1*. Risk score analysis using associated SNPs showed a tenfold increased risk of myopia for subjects with the highest genetic load. Our results, accumulated across independent multi-ethnic studies, considerably advance understanding of mechanisms involved in refractive error and myopia.

Refractive error is the most important cause of visual impairment in the world[1]. Myopia, or nearsightedness, in particular is associated with structural changes of the eye, increasing the risk of severe complications such as macular degeneration, retinal detachment, and glaucoma. The prevalence of myopia has been rising dramatically over the past few decades[2], and it is estimated that 2.5 billion people will be affected by myopia within a decade[3]. Although several genetic loci influencing refractive error have been identified[4-10], their contribution to phenotypic variance is small, and many more loci are expected to explain its genetic architecture.

Here the Consortium for Refractive Error and Myopia (CREAM) presents results from the largest international genome-wide meta-analysis on refractive error with data from 32

studies from Europe, the United States, Australia, and Asia. The meta-analysis was performed in three stages: as a first step, we investigated genome-wide association study (GWAS) results of 37,382 individuals from 27 populations of European ancestry (Supplementary Note, Supplementary Table 1) using spherical equivalent as a continuous outcome; as a second step, we aimed to test cross-ethnic transferability of the statistical significant associations from the first stage in 8,376 individuals from 5 Asian cohorts (Supplementary Note, Supplementary Table 1). As a third step, we performed a GWAS meta-analysis on the combined populations (total n = 45,758). Subsequently, we examined the influence of associated alleles on the risk of myopia in a genetic risk score analysis, and lastly, we evaluated gene expression in ocular tissues and explored potential mechanisms by which newly found loci may exert their effect on refractive development.

At step 1, we analyzed ~2.5 million autosomal single nucleotide polymorphisms (SNPs) which were obtained through whole-genome imputation of genotypes to HapMap 2. The inflation factors (γ_{GC}) of the test statistics in individual studies contributing to the meta-analysis ranged between 0.992 and 1.050, indicating excellent within-study control of population substructure (Supplementary Table 2). The overall lambda was 1.09, consistent with a polygenic inheritance model for refractive error (Q-Q plot, Supplementary Figure S1). We did not perform a lambda correction as Yang et al. have shown that in this situation substantial genomic inflation can be expected, even in the absence of population structure and technical artifacts[11]. We identified 309 SNPs that exceeding the conventional genome-wide significance threshold of $P=5.0\times10^{-8}$ in the European ancestry sample. These SNPs were clustered in 18 distinct genomic regions across 14 chromosomes (Figure 1, Table 1). At step 2, we investigated the 18 best associated SNPs in the Asian population: ten showed evidence of association (Table 1). The most significant association in both ancestry groups was at a previously identified locus on chromosome 15q14 in the proximity of the *GJD2* gene (SNP rs524952; $P_{combined}=1.44\times10^{-15}$)[4,12]. The locus near the *RASGRF1* gene was also replicated in the meta-analysis (SNP rs4778879; $P_{combined}=4.25\times10^{-11}$)[9], the remaining 16 genome-wide significantly associated loci had not previously been reported in association with refractive error. Those loci that were not significant in the smaller sized Asian population mostly had a similar effect size and direction of effect as in the European ancestry sample. At step 3, we identified 8 additional loci which exceeded genome-wide significance in the combined analysis (Table 2). Regional and forest plots of the associated loci are provided in Supplementary Figures 2 and 3.

Genotype distributions of the risk alleles were evaluated in Rotterdam Studies 1-3 (n=9,307). The clinical utility for the prediction of risk of myopia was evaluated by a weighted genetic risk score analysis based on the aggregate of effects (regression coefficients betas) of individual SNPs derived from the meta-analysis, using the middle risk category as a reference. Risk scores ranged from a mean risk score of 1.88 (95% CI 1.86 - 1.89) in the lowest risk score category to 3.63 (95% CI 3.61-3.65) in the highest risk score category. Having the lowest or the highest genetic risk score was associated with an odds ratio of 0.38 (95% CI 0.18-0.77), and an odds ratio of 10.97 (95% CI 3.727-31.251) of myopia, respectively (Figure 2). The predictive value (area under receiver operating characteristic curve, AUC) of myopia versus hyperopia was 0.67 (95% CI 0.65-0.69), a relatively high value for genetic factors in a complex trait[13,14]. The genetic variants explain 3.4% of the phenotypic variation in refractive error in the Rotterdam Study.

We examined the expression of genes harboring a genetic association signal by measuring levels of RNA in various eye tissues, and found most of these genes expressed in the eye (Supplementary Table 3). The genes *PRSS56, LOC100506035*, and *SHISA6* were not available in the expression data set; all other genes were expressed in the retina. Subsequently, we assessed the areas where our SNP hits reside for H3K27ac modification

marks[15], and HaploReg[16] annotations for marks of active regulatory elements (Supplementary Table 4, Supplementary Figure 4). We found that many hits contain these elements, and alteration of regulatory function is therefore a suggestive mechanism.

The widely-accepted model for myopia development is that eye growth is triggered by a visually-evoked signaling cascade, which originates from the sensory retina, traverses the retinal pigment epithelium and choroid, and terminates in the sclera, where active extracellular matrix (ECM) remodeling results in a relative elongation of the eye[17]. Many of the genes in or near the identified loci can be linked to biological processes that drive this cascade. Neurotransmission in the retina is a necessary mechanism for eye growth regulation; the most significantly associated gene *GJD2* plays a role herein. This gene forms a gap junction between neuronal cells in the retina, enabling intracellular exchange of small molecules and ions. The other previously-reported gene *RASGRF1* is a nuclear exchange factor that promotes GDP/GTP exchange on Ras-family GTPases, and is involved in synaptic transmission of photoreceptor responses[18,19]. Both *GJD2* and *RASGRF1* knockout mice show retinal photoreception defects[18,20]. One of the newly identified genes, *GRIA4* (SNP rs11601239; $P_{combined}=5.92\times10^{-9}$) also has a potential function in this pathway. This gene is a glutamate-gated ion channel that mediates fast synaptic excitatory neurotransmission[21], is present in various retinal cells[22], has been shown to be critical for light signaling in the retina[23] and emmetropization[24]. Another gene involved in synaptic transmission is *A2BP1* (also known as *RBFOX1*; SNP rs17648524; $P_{combined}=5.64\times10^{-10}$, an RNA-binding splicing regulator which modulates membrane excitability[25].

We identified for the first time a number of genes involved in ion transport, channel activity and maintenance of membrane potential. *KCNQ5*, a potassium channel regulator (SNP rs7744813; $P_{combined}=4.18\times10^{-9}$), participates in the transport of K^+ from the retina to the choroid, and may contribute to voltage-gated K^+ channels in photoreceptors and retinal neurons associated with myopia[26,27]. *CD55* (SNP rs1652333; $P_{combined}=3.05\times10^{-12}$) is known to elevate cytosolic calcium ion concentration. Other ion channel genes include *CACNA1D*, a voltage-sensitive calcium channel regulator; *KCNJ2*, a regulator of potassium ion transport; *CHRNG*, a nicotinic cholinergic receptor; and *MYO1D*, a putative binder of calmodulin, which mediates Ca^+ sensitivity to KCNQ5 ion channels.

Retinoic acid is synthesized in the retina and highly expressed in the choroid and has been implicated in eye growth in experimental myopia models[28-30]. Retinol dehydrogenase 5 (*RDH5)*, a novel refractive error susceptibility gene (SNP rs3138144; $P_{combined}=4.44\times10^{-12}$), is involved in the recycling of 11-cis-retinal in the visual cycle[31]. Mutations in *RDH5* cause congenital stationary night blindness (OMIM# 136880), a disease associated with myopia. Other genes involved in retinoic acid metabolism are *RORB* (RAR-related orphan receptor), and *CYP26A1*, genes that were significant in the European ancestry studies. Notably, retinoic acid contributes to ECM remodeling by regulating cell differentiation.

ECM remodeling of the sclera is the pathological hallmark in myopia development. *LAMA2* (*laminin α2*, SNP rs12205363; $P_{combined}=1.79\times10^{-12}$) is the most prominent gene in this respect. *LAMA2* forms a subunit of the heterotrimer laminins which are essential components of basement membranes, stabilizing cellular structures and facilitating cell migration[32]. The two bone morphogenic genes (*BMP2*, SNP rs235770; $P_{combined}=1.57\times10^{-8}$; *BMP3*) can also be placed within the ECM architecture. They are members of the transforming growth factor-β (TGFβ) super-family, regulate growth and differentiation of mesenchymal cells, and may orchestrate the organization of other connective tissues than bone such as sclera. Remarkably, *BMP2* shows bidirectional expression in retinal pigment epithelium in myopia animal models[33].

Genes involved in eye development appeared as a separate entity among the gene functions. *SIX6* (SNP rs1254319; $P_{combined}=1.00\times10^{-8}$ has been linked to anophthalmia and glaucoma[34,35], *PRSS56 (protease serine 56*, SNP rs1656404; $P_{combined}=7.86\times10^{-11}$) to microphthalmia[36-38], *CHD7* to CHARGE syndrome, a congenital condition with severe eye structural defects, and *ZIC2* to brain development including visual perception. For the remaining novel gene associations, a mechanism in the pathogenesis of myopia is not immediately clear. Results from Ingenuity and the Protein Link Evaluator[39] (Supplementary Figure 5) visualize the subcellular location of all associated genes, and illustrates their interrelationships. Direct connections between genes were surprisingly infrequent, suggesting molecular disease heterogeneity or functional redundancy in the pathobiological events involved in development of refractive error and myopia.

In summary, we identified 24 new chromosomal loci associated with refractive error through a large-scale meta-analysis of GWAS from international multi-ethnic studies. The significant overlap in genetic loci for refractive error between subjects of European ancestry and Asians provides evidence for shared genetic risk factors between the populations. The tenfold increased risk of myopia for those carrying the highest number of risk alleles depicts the clinical significance of our findings. Further elucidation of the mechanisms by which these loci affect eye growth carries the potential to improve the visual outcome of this common trait.

Online methods

Study design

We performed a meta-analysis on directly genotyped and imputed SNPs from individuals of European ancestry in 27 studies, with a total of 37,382 individuals. Subsequently, we evaluated significant SNPs in 8,376 subjects of Asian origin from 5 different studies, and performed a meta-analysis on all studies combined.

Subjects and phenotyping

All studies participating in this meta-analysis are part of the Consortium for Refractive Error and Myopia (CREAM). All studies had a population-based design and had a similar protocol for phenotyping (Supplementary Table 1). Eligible participants underwent a complete ophthalmologic examination including a non-dilated measurement of refractive error of both eyes. Exclusion criteria were all conditions that could alter refraction, such as cataract surgery, laser refractive procedures, retinal detachment surgery, keratoconus, or ocular or systemic syndromes. Inclusion criteria were persons aged 25 years and over who had data on refractive error and genotype.

The meta-analysis of step 1 was based on 27 studies of European ancestry: 1958 British Birth Cohort, ALSPAC, ANZRAG, AREDS1a1b, AREDS1c, CROATIA-Korcula, CROATIA-Split, CROATIA-Vis, EGCUT, FECD, TEST/BATS, FITSA, Framingham, GHS 1, GHS 2, KORA, ORCADES, TwinsUK, WESDR, YFS, ERF, DCCT, BMES, RS1, RS2, RS3, and OGP Talana. The second step was formed by 5 Asian studies: Beijing Eye Study, SCES, SIMES, SINDI, and SP2.

General methods, demographics and phenotyping and genotyping methods of the study cohorts can be found in the Supplementary Note and Supplementary Table 1. All studies were performed with the approval of their local Medical Ethics Committee, and written informed consent was obtained from all participants in accordance with the Declaration of Helsinki.

Genotyping and imputation

Particulars of genotyping in each cohort, particular platforms used to generate genotyping and methods of imputation can be found in more detail in the Supplementary Table 5. To produce consistent datasets and enable meta-analysis of studies across different genotyping platforms, the cohorts performed genomic imputation on the HapMap Phase 2 available genotypes with MACH[40] or IMPUTE[41], using the appropriate ancestry as templates.

Each cohort applied stringent quality control procedures prior to the imputation, including minor allele frequency cutoffs, Hardy-Weinberg equilibrium ($P > 10^{-7}$), genotypic success rate (>95%), Mendelian inconsistencies, exclusion of individuals with more than 5% shared ancestry (exception made for family-based cohorts in which due adjustment for family relationship was made) and removal of all individuals whose ancestry as determined through genetic analysis did not match the prevailing ancestry group of the own cohort. SNPs with low imputation quality were filtered using metrics specific to the imputation method and thresholds used in their previous GWAS analyses. Hence, imputation quality criteria varied slightly among studies, and low-confidence imputed SNPs were omitted in the meta-analysis for individual studies.

Statistical analysis

Spherical equivalent was calculated according to the standard formula (SE=sphere + ½ cylinder), and the mean of two eyes was used for analysis. When data from only one eye was available, the SE of this eye was used.

Each cohort performed association analyses in which the spherical equivalent (determined as described above) was the dependent variable and genotypes (number of alleles in each of the HapMap2 loci) as the independent variables. Analyses in all cases also adjusted for sex and age at the time of phenotype measurement. In family-based cohorts score-test based association test was used to adjust for within-family relatedness (see Supplementary Note)[42,43]. Study-specific lambda estimates are shown in Supplementary Table 2.

All study effect estimates were corrected using genomic control and were oriented to the positive strand of the NCBI build 36 reference sequence of the human genome, which was the genomic build on which most available genotyping platforms were based. The coordinates and further annotations of the SNPs were further converted into build 37, the most recent of the available builds at the time of writing.

Meta-analyses used effect size estimations (beta regression coefficients) and standard errors from individual cohorts' summary statistics. Random-effects were assumed for all the meta-analyses which were performed using GWAMA[44]. We tested for heterogeneous effects between the two ancestries using METAL[45] for Linux. For the purpose of these analyses, we defined significance as equal to or better than the conventional multiple testing genome-wide thresholds of association ($P<5.0 \times 10^{-8}$) for stage 1 and nominally significant probabilities ($P<0.05$) for stage 2. Manhattan, regional plots and forest plots were made using R (see **URLs**) and Locuszoom (see **URLs**)[46].

For the Rotterdam Study 1-3, a weighted genetic risk score per individual was calculated using the regression coefficients from the GWAS meta-analysis model for the association of SNPs within the associated 26 loci (Table 1, Table 2; per locus only one SNP was included in the analysis) and the individual allele dosages per genotype to evaluate the relationships between myopia (SE ≤ − 3 D), emmetropia (−1.5 D ≤ SE ≤ 1.5 D) and hyperopia (SE ≥ +3 SD). The weighted risk scores were categorized and mean odds ratios per risk score category were calculated for subjects with myopia versus hyperopia, using the middle risk score category as a reference. Subsequently, the area under the receiver curve (AUC) was

calculated for myopia versus emmetropia and myopia versus hyperopia. Lastly, the proportion of variance of spherical equivalent explained by the identified SNPs was calculated. For these analyses, we used SPSS version 20.0.0 (SPSS Inc.).

Gene expression data in human eye tissue

Independently designed, collected, and reported human ocular tissue array data from two different sources, as well as literature reviews were used to verify evidence of expression of the candidate genes.

RPE, photoreceptors and choroid

Human gene expression data of RPE, photoreceptors and choroid were obtained essentially as described[47] and the dataset has been deposited in NCBI's Gene Expression Omnibus[48] (GEO series accession number GSE20191; see **URLs**). In short, postmortem eye bulbs (retinal pigment epithelium was obtained from six donor eyes, choroid was obtained from three donor eyes and photoreceptors were obtained from three donor eyes), provided by the Corneabank Amsterdam, were rapidly frozen using liquid nitrogen. Donors were between 63 and 78 years old and had no known history of eye pathology. Cryosections were cut from the macula, and histology was used to confirm a normal histological appearance. Retinal pigment epithelium, photoreceptor and choroidal cells were isolated from macular sections using a Laser Microdissection System (PALM). Total RNA was isolated and the mRNA component was amplified, labeled and hybridized to a 44K microarray (Agilent Technologies)[49]. At least three to six microarrays were performed per tissue. Sample isolation, procedures and expression microarray analysis were carried out according to MIAMI guidelines. As a measure of the level of expression, we sorted all the genes represented on the 44K microarray by increasing their expression, and we calculated the corresponding percentiles (Supplementary Table 3a).

Sclera, cornea and optic nerve

We assessed expression of the associated genes in sclera, cornea and optic nerve tissue in an additional dataset (unpublished data). Adult eyes were obtained from the North Carolina Eye Bank (Winston-Salem, North Carolina). All whole globes were immersed in RNALater (Quiagen, Hilden, Germany) within 6.5 hours of collection, shipped overnight on ice, and dissected on the day of arrival. The retina, choroid and scleral tissues were isolated at the posterior pole using a circular, double embedded technique using round 7 mm and 5 mm biopsy punches. To reduce contamination of retina to the other ocular tissues samples, the second biopsy punch of 5 mm was used in the center of the 7 mm punch after retinal removal. RNA samples (quality control of RNA concentration and 260/280 nm ratios using Nanodrop®) (Invitrogen, Carlsbad, California, USA) were hybridized to whole genome microaray Illumina® HumanHT-12 v4 Expression BeadChips (over 25,000 genes and 48,000 probes) in two batches. The first batch was hybridized to adult RPE, choroid, and sclera RNA samples (n=6). The second batch of newer chips with additional probes was hybridized to adult optic nerve and cornea samples (n=6). The data were exported from Illumina® GenomeStudio and log2 transformed. Sample outliers were determined by principle component analyses using the Hoteling's T2 test[50] (at 95% confidence interval) and removed from further analyses. The data intensity was normalized by Quantile normalization followed by Multichip Averaging[51] to reduce chip effects. For each tissue type, the probes with signal intensities below background levels and those with the lowest (5%) signal intensities (detection $P<0.10$) were excluded. Evidence of expression in the remaining probes was defined by detection $P<0.05$. Probes with detection P values < 0.10 and > 0.05 required additional tissue expression support from EyeSAGE or literature reports (Supplementary Table 3b).

Search for regulatory elements

We used the 'Integrated Regulation from ENCODE' track in the UCSC genome browser to look at H3K27ac modificiation marks as a mark of active regulatory elements. Numbers of H3K27ac modification marks were counted between the associated topSNP from a locus and the nearest gene and within (the nearest) gene itself. We also used HaploReg[16] annotations to look for other signs of regulatory activity at the site of the associated SNP itself, such as enhancer histone marks, DNAse hypersensitivity sites, binding proteins and motifs changed.

Pathway analyses

We used two different programs for pathway analsysis; Ingenuity (see **URLs**), version August 2012, application build 172788, content version 14197757) and the Disease Association Protein-Protein Link Evaluator (DAPPLE)[39].

Subcellular localization assignment and functional annotation of myopia associated disease genes as well as molecular pathway analysis was carried out using the Ingenuity knowledge database. The candidate myopia disease genes discovered in this study were entered into the Ingenuity knowledge database (IPA). We used the "IPA toggle subcellular layout" function to show the subcellular location (extracellular, plasma membrane, cytoplasm, nucleus, unknown) of the proteins corresponding to these genes, which yield a first glance which signaling molecules and pathways are involved in myopia. Subsequently, we used the IPA "connect" function to discover potential direct or indirect functional relationships or molecular pathways in between these entries. This yielded surprisingly little hits, which suggest molecular disease heterogeneity and/or functional redundancy in the pathobiological events leading to myopia. Next, we used the IPA "overlay" function to annotate the myopia candidate disease genes with (their involvement in) "functions and diseases", "canonical pathways" and a range of custom made gene lists from previous studies, including photoreceptor, RPE, and choroidal specific transcripts (partly published[52]). Lastly, we used the Disease Association Protein-Protein Link Evaluator (DAPPLE)[39] to look for physical connections between proteins encoded from disease-genes associated regions.

Supplementary Material

Refer to Web version on PubMed Central for supplementary material.

Acknowledgments

We gratefully thank the invaluable contributions of all study participants, their relatives and staff at the recruitment centers. Complete funding information and acknowledgements per study can be found in the Supplementary Note.

References

1. Wojciechowski R. Nature and nurture: the complex genetics of myopia and refractive error. Clin Genet. 2011; 79:301–20. [PubMed: 21155761]
2. Mutti DO, et al. Axial growth and changes in lenticular and corneal power during emmetropization in infants. Invest Ophthalmol Vis Sci. 2005; 46:3074–80. [PubMed: 16123404]
3. Smith TS, Frick KD, Holden BA, Fricke TR, Naidoo KS. Potential lost productivity resulting from the global burden of uncorrected refractive error. Bull World Health Organ. 2009; 87:431–7. [PubMed: 19565121]
4. Solouki AM, et al. A genome-wide association study identifies a susceptibility locus for refractive errors and myopia at 15q14. Nat Genet. 2010; 42:897–901. [PubMed: 20835239]
5. Shi Y, et al. Genetic variants at 13q12.12 are associated with high myopia in the Han Chinese population. Am J Hum Genet. 2011; 88:805–13. [PubMed: 21640322]

6. Nakanishi H, et al. A genome-wide association analysis identified a novel susceptible locus for pathological myopia at 11q24.1. PLoS Genet. 2009; 5:e1000660. [PubMed: 19779542]
7. Li Z, et al. A genome-wide association study reveals association between common variants in an intergenic region of 4q25 and high-grade myopia in the Chinese Han population. Hum Mol Genet. 2011; 20:2861–8. [PubMed: 21505071]
8. Li YJ, et al. Genome-wide association studies reveal genetic variants in CTNND2 for high myopia in Singapore Chinese. Ophthalmology. 2011; 118:368–75. [PubMed: 21095009]
9. Hysi PG, et al. A genome-wide association study for myopia and refractive error identifies a susceptibility locus at 15q25. Nat Genet. 2010; 42:902–5. [PubMed: 20835236]
10. Fan Q, et al. Genetic variants on chromosome 1q41 influence ocular axial length and high myopia. PLoS Genet. 2012; 8:e1002753. [PubMed: 22685421]
11. Yang J, et al. Genomic inflation factors under polygenic inheritance. Eur J Hum Genet. 2011; 19:807–12. [PubMed: 21407268]
12. Verhoeven VJ, et al. Large scale international replication and meta-analysis study confirms association of the 15q14 locus with myopia. The CREAM consortium. Hum Genet. 2012; 131:1467–80. [PubMed: 22665138]
13. Speliotes EK, et al. Association analyses of 249,796 individuals reveal 18 new loci associated with body mass index. Nat Genet. 2010; 42:937–48. [PubMed: 20935630]
14. Estrada K, et al. Genome-wide meta-analysis identifies 56 bone mineral density loci and reveals 14 loci associated with risk of fracture. Nat Genet. 2012; 44:491–501. [PubMed: 22504420]
15. Consortium EP, et al. An integrated encyclopedia of DNA elements in the human genome. Nature. 2012; 489:57–74. [PubMed: 22955616]
16. Ward LD, Kellis M. HaploReg: a resource for exploring chromatin states, conservation, and regulatory motif alterations within sets of genetically linked variants. Nucleic Acids Res. 2012; 40:D930–4. [PubMed: 22064851]
17. Rymer J, Wildsoet CF. The role of the retinal pigment epithelium in eye growth regulation and myopia: a review. Vis Neurosci. 2005; 22:251–61. [PubMed: 16079001]
18. Fernandez-Medarde A, et al. RasGRF1 disruption causes retinal photoreception defects and associated transcriptomic alterations. J Neurochem. 2009; 110:641–52. [PubMed: 19457086]
19. Tonini R, et al. Expression of Ras-GRF in the SK-N-BE neuroblastoma accelerates retinoic-acid-induced neuronal differentiation and increases the functional expression of the IRK1 potassium channel. Eur J Neurosci. 1999; 11:959–66. [PubMed: 10103089]
20. Abd-El-Barr MM, et al. Genetic dissection of rod and cone pathways in the dark-adapted mouse retina. J Neurophysiol. 2009; 102:1945–55. [PubMed: 19587322]
21. Beyer B, et al. Absence seizures in C3H/HeJ and knockout mice caused by mutation of the AMPA receptor subunit Gria4. Hum Mol Genet. 2008; 17:1738–49. [PubMed: 18316356]
22. Connaughton, V. Glutamate and Glutamate Receptors in the Vertebrate Retina. In: Kolb, H.; Fernandez, E.; Nelson, R., editors. Webvision: The Organization of the Retina and Visual System. Salt Lake City (UT): 1995.
23. Yang J, Nemargut JP, Wang GY. The roles of ionotropic glutamate receptors along the On and Off signaling pathways in the light-adapted mouse retina. Brain Res. 2011; 1390:70–9. [PubMed: 21406186]
24. Smith EL 3rd, Fox DA, Duncan GC. Refractive-error changes in kitten eyes produced by chronic on-channel blockade. Vision Res. 1991; 31:833–44. [PubMed: 2035267]
25. Fogel BL, et al. RBFOX1 regulates both splicing and transcriptional networks in human neuronal development. Hum Mol Genet. 2012; 21:4171–86. [PubMed: 22730494]
26. Zhang X, Yang D, Hughes BA. KCNQ5/K(v)7.5 potassium channel expression and subcellular localization in primate retinal pigment epithelium and neural retina. Am J Physiol Cell Physiol. 2011; 301:C1017–26. [PubMed: 21795522]
27. Pattnaik BR, Hughes BA. Effects of KCNQ channel modulators on the M-type potassium current in primate retinal pigment epithelium. Am J Physiol Cell Physiol. 2012; 302:C821–33. [PubMed: 22135213]

28. Troilo D, Nickla DL, Mertz JR, Summers Rada JA. Change in the synthesis rates of ocular retinoic acid and scleral glycosaminoglycan during experimentally altered eye growth in marmosets. Invest Ophthalmol Vis Sci. 2006; 47:1768–77. [PubMed: 16638980]
29. Mertz JR, Wallman J. Choroidal retinoic acid synthesis: a possible mediator between refractive error and compensatory eye growth. Exp Eye Res. 2000; 70:519–27. [PubMed: 10866000]
30. McFadden SA, Howlett MH, Mertz JR. Retinoic acid signals the direction of ocular elongation in the guinea pig eye. Vision Res. 2004; 44:643–53. [PubMed: 14751549]
31. Parker RO, Crouch RK. Retinol dehydrogenases (RDHs) in the visual cycle. Exp Eye Res. 2010; 91:788–92. [PubMed: 20801113]
32. Scheele S, et al. Laminin isoforms in development and disease. J Mol Med (Berl). 2007; 85:825–36. [PubMed: 17426950]
33. Zhang Y, Liu Y, Wildsoet CF. Bidirectional, Optical Sign-Dependent Regulation of BMP2 Gene Expression in Chick Retinal Pigment Epithelium. Invest Ophthalmol Vis Sci. 2012; 53:6072–80. [PubMed: 22879416]
34. Ramdas WD, et al. A genome-wide association study of optic disc parameters. PLoS Genet. 2010; 6:e1000978. [PubMed: 20548946]
35. Gallardo ME, et al. Analysis of the developmental SIX6 homeobox gene in patients with anophthalmia/microphthalmia. Am J Med Genet A. 2004; 129A:92–4. [PubMed: 15266624]
36. Gal A, et al. Autosomal-recessive posterior microphthalmos is caused by mutations in PRSS56, a gene encoding a trypsin-like serine protease. Am J Hum Genet. 2011; 88:382–90. [PubMed: 21397065]
37. Orr A, et al. Mutations in a novel serine protease PRSS56 in families with nanophthalmos. Mol Vis. 2011; 17:1850–61. [PubMed: 21850159]
38. Nair KS, et al. Alteration of the serine protease PRSS56 causes angle-closure glaucoma in mice and posterior microphthalmia in humans and mice. Nat Genet. 2011; 43:579–84. [PubMed: 21532570]
39. Rossin EJ, et al. Proteins encoded in genomic regions associated with immune-mediated disease physically interact and suggest underlying biology. PLoS Genet. 2011; 7:e1001273. [PubMed: 21249183]
40. Li Y, Willer CJ, Ding J, Scheet P, Abecasis GR. MaCH: using sequence and genotype data to estimate haplotypes and unobserved genotypes. Genet Epidemiol. 2010; 34:816–34. [PubMed: 21058334]
41. Marchini J, Howie B, Myers S, McVean G, Donnelly P. A new multipoint method for genome-wide association studies by imputation of genotypes. Nat Genet. 2007; 39:906–13. [PubMed: 17572673]
42. Aulchenko YS, Struchalin MV, van Duijn CM. ProbABEL package for genome-wide association analysis of imputed data. BMC Bioinformatics. 2010; 11:134. [PubMed: 20233392]
43. Chen WM, Abecasis GR. Family-based association tests for genomewide association scans. Am J Hum Genet. 2007; 81:913–26. [PubMed: 17924335]
44. Magi R, Morris AP. GWAMA: software for genome-wide association meta-analysis. BMC Bioinformatics. 2010; 11:288. [PubMed: 20509871]
45. Willer CJ, Li Y, Abecasis GR. METAL: fast and efficient meta-analysis of genomewide association scans. Bioinformatics. 2010; 26:2190–1. [PubMed: 20616382]
46. Pruim RJ, et al. LocusZoom: regional visualization of genome-wide association scan results. Bioinformatics. 2010; 26:2336–7. [PubMed: 20634204]
47. Booij JC, et al. Functional annotation of the human retinal pigment epithelium transcriptome. BMC Genomics. 2009; 10:164. [PubMed: 19379482]
48. Edgar R, Domrachev M, Lash AE. Gene Expression Omnibus: NCBI gene expression and hybridization array data repository. Nucleic Acids Res. 2002; 30:207–10. [PubMed: 11752295]
49. van Soest SS, et al. Comparison of human retinal pigment epithelium gene expression in macula and periphery highlights potential topographic differences in Bruch's membrane. Mol Vis. 2007; 13:1608–17. [PubMed: 17893662]

50. Hotelling H. The Generalization of Student's Ratio. The Annals of Mathematical Statistics. 1931; 2:360–378.

51. Irizarry RA, et al. Exploration, normalization, and summaries of high density oligonucleotide array probe level data. Biostatistics. 2003; 4:249–64. [PubMed: 12925520]

52. Booij JC, et al. A new strategy to identify and annotate human RPE-specific gene expression. PLoS One. 2010; 5:e9341. [PubMed: 20479888]

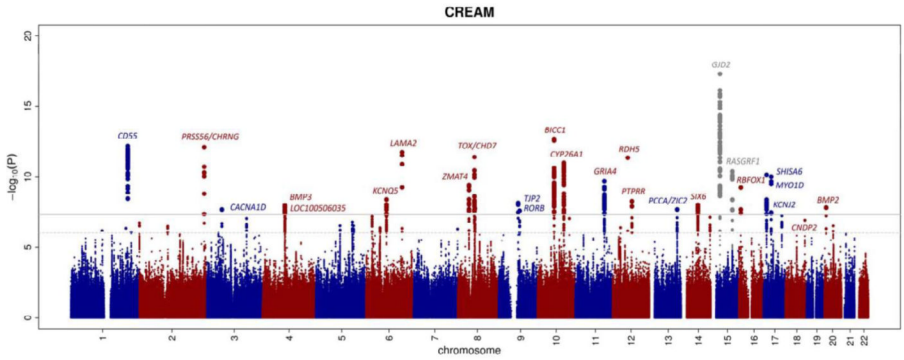

Figure 1. Manhattan plot of the GWAS meta-analysis for refractive error in the combined analysis (n = 45,758)

The plot shows −log10-transformed *P* values for all SNPs; the upper horizontal line represents the genome-wide significance threshold of $P < 5.0 \times 10^{-8}$; the lower line indicates *P* value of 10^{-5}. Previously reported genes are depicted in grey. The *A2BP1* gene is also known as *RBFOX1.*

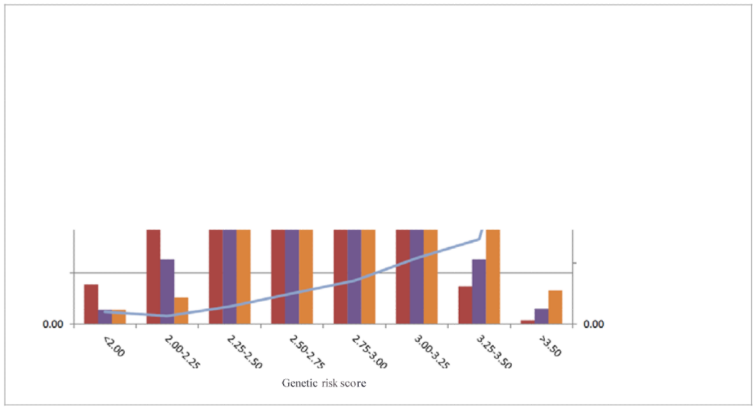

Figure 2. Genetic risk score for myopia

Distribution of subjects from Rotterdam Study 1-3 (n= 9,307) with myopia (SE ≤ −3 D), emmetropia (SE ≥ −1.5 D & ≤ 1.5 D) and hyperopia (SE ≥ 3 D) as a function of genetic risk score. This score is based on the regression coefficients and allele dosages of the associated SNPs for all 26 loci identified in the meta-analysis. The mean OR of myopia was calculated per risk category, using the middle risk score category (risk score 2.50; 2.75) as a reference.

Table 1

Genome-wide significant hits for refractive error in the European ancestry population with results in Asian population and combined analysis

Summary of SNPs that showed genome-wide significant (P<5×10-8) association with spherical equivalent (SE) in subjects of European ancestry (stage 1), with results of replication in Asians (stage 2) and combined analysis (stage 3). Previously reported genes are marked in grey. We tested for heterogeneous effects between the Asian and the European ancestry sample, for which *P* values are shown. Abbreviations: SNP, single nucleotide polymorphism; Nearest gene, reference NCBI build 37; A1, reference allele; A2, other allele, MA, Minor Allele; MAF, average Minor Allele Frequency; Beta, effect size on spherical equivalent in diopters based on allele A1; SEM, standard error of the mean.

Number of loci	SNP	Chromosome	Position	Nearest gene	A1/A2	MAF	Beta	SEM	P value	MAF	Beta	SEM	P value	Beta	SEM	P value	P value
						Stage 1 (n = 37,382)				*Stage 2 (n = 8,376)*				*Combined (n = 45,758)*			*Heterogeneity*
1	rs1652333	1	203858855	*CD55*	G/A	0.32	−0.115	0.018	6.29E-11	0.42	−0.099	0.035	5.00E-03	−0.112	0.016	3.05E-12	0.94
2	rs1656404	2	233205446	*PRSS56*	A/G	0.21	−0.151	0.025	2.38E-09	0.11	−0.167	0.069	1.60E-02	−0.153	0.024	7.86E-11	0.83
	rs1881492	2	233406997	*CHRNG*	T/G	0.22	−0.145	0.022	1.28E-10	0.15	−0.057	0.110	6.09E-01	−0.139	0.021	5.15E-11	0.88
3	rs14165	3	53847407	*CACNA1D*	A/G	0.32	0.095	0.017	4.36E-08	0.12	0.120	0.100	2.29E-01	0.096	0.017	2.14E-08	0.25
4	rs1960445	4	81930813	*BMP3*	C/T	0.17	−0.147	0.026	1.19E-08	0.11	0.034	0.055	5.32E-01	−0.114	0.024	1.25E-06	0.31
5	rs12205363	6	129834628	*LAMA2*	C/T	0.10	0.228	0.034	1.13E-11	0.02	0.553	0.236	1.92E-02	0.235	0.033	1.79E-12	0.93
6	rs4237036	8	61701056	*CHD7*	C/T	0.35	0.097	0.017	1.52E-08	0.23	0.043	0.040	2.81E-01	0.089	0.016	1.82E-08	0.76
	rs7837791	8	60179085	*TOX*	T/G	0.49	0.106	0.017	9.22E-10	0.39	0.103	0.035	4.00E-03	0.106	0.015	3.99E-12	0.70
7	rs7829127	8	40726393	*ZMAT4*	G/A	0.25	0.116	0.020	3.04E-09	0.11	0.112	0.055	4.23E-02	0.116	0.018	3.69E-10	0.66
8	rs7042950	9	77149836	*RORB*	G/A	0.24	−0.113	0.020	1.02E-08	0.42	−0.040	0.037	2.72E-01	−0.096	0.018	4.15E-08	0.83
9	rs10882165	10	94924323	*CYP26A1*	T/A	0.42	−0.111	0.016	1.25E-11	0.20	−0.060	0.056	2.84E-01	−0.107	0.016	1.03E-11	0.90
10	rs7084402	10	60265403	*BICC1*	G/A	0.48	−0.111	0.016	7.23E-12	0.50	−0.094	0.035	7.34E-03	−0.108	0.015	2.06E-13	0.71
11	rs11601239	11	105061808	*GRIA4*	C/G	0.46	−0.092	0.017	3.45E-08	0.42	−0.129	0.058	2.70E-02	−0.095	0.016	5.92E-09	0.83
12	rs3138144	12	56114768	*RDH5*	C/G	0.48	0.113	0.018	4.28E-10	0.45	0.157	0.072	3.00E-02	0.119	0.017	4.44E-12	0.09
13	rs2184971	13	100818091	*PCCA*	G/A	0.44	0.095	0.016	5.90E-09	0.22	0.022	0.040	5.84E-01	0.085	0.015	2.11E-08	0.96
	rs8000973	13	100691366	*ZIC2*	T/C	0.47	0.089	0.016	4.24E-08	0.22	0.030	0.041	4.63E-01	0.081	0.015	5.10E-08	0.50
14	rs524952	15	35005885	*GJD2*	A/T	0.48	−0.154	0.021	1.11E-13	0.44	−0.193	0.060	1.00E-03	−0.158	0.020	1.44E-15	0.22
15	rs4778879	15	79372874	*RASGRF1*	G/A	0.44	−0.103	0.017	1.27E-09	0.39	−0.103	0.043	1.50E-02	−0.102	0.015	4.25E-11	0.15
16	rs17183295	17	31078271	*MYO1D*	T/C	0.23	−0.132	0.021	3.04E-10	0.16	−0.166	0.144	2.49E-01	−0.131	0.020	9.66E-11	0.34
17	rs4793501	17	68718733	*KCNJ2*	C/T	0.42	0.096	0.016	3.21E-09	0.44	0.010	0.034	7.64E-01	0.080	0.014	2.79E-08	0.04
18	rs12971120	18	72174022	*CNDP2*	G/A	0.23	0.108	0.020	4.39E-08	0.30	0.014	0.063	8.27E-01	0.099	0.019	1.85E-07	0.49

Table 2

Additional genome-wide significant hits from the combined meta-analysis (n = 45,758)

Summary of SNPs that showed genome-wide significant (P<5×10-8) association with spherical equivalent (SE) in the combined analysis (stage 3), with results in subjects of European ancestry (stage 1) and Asians (stage 2). We tested for heterogeneous effects between the two ancestries, for which *P* values are shown. Abbreviations: SNP, single nucleotide polymorphism; Nearest gene, reference NCBI build 37; A1, reference allele; A2, other allele, MA, Minor Allele; MAF, average Minor Allele Frequency; Beta, effect size on spherical equivalent in diopters based on allele A1; SEM, standard error of the mean. The *A2BP1* gene is also known as *RBFOX1.*

Number of loci	SNP	Chromosome	Position	Nearest gene	A1/A2	Beta	SEM	P value	MAF	Beta	SEM	P value	MAF	Beta	SEM	P value	P value
						Combined (n = 45,758)				*Stage 1 (n = 37,382)*				*Stage 2 (n = 8,376)*			*Heterogeneity*
1	rs9307551	4	80530670	*LOC100506035*	A/C	−0.099	0.017	1.09E-08	0.25	−0.097	0.020	1.37E-06	0.50	−0.105	0.035	3.06E-03	0.70
2	rs7744813	6	73643288	*KCNQ5*	C/A	0.112	0.019	4.18E-09	0.41	0.114	0.021	6.80E-08	0.33	0.094	0.046	4.30E-02	0.14
3	rs11145465	9	71766592	*TJP2*	A/C	−0.124	0.021	7.26E-09	0.25	−0.125	0.023	6.92E-08	0.07	−0.136	0.091	1.35E-01	0.14
4	rs12229663	12	71249995	*PTPRR*	G/A	0.099	0.017	5.47E-09	0.27	0.104	0.019	5.46E-08	0.36	0.080	0.052	1.23E-01	0.74
5	rs1254319	14	60903756	*SIX6*	A/G	−0.088	0.015	1.00E-08	0.32	−0.088	0.017	2.03E-07	0.34	−0.087	0.036	1.57E-02	0.59
6	rs17648524	16	7459682	*A2BP1*	C/G	−0.118	0.019	5.64E-10	0.36	−0.116	0.022	7.48E-08	0.14	−0.140	0.058	1.60E-02	0.24
7	rs2969180	17	11407900	*SHISA6*	A/G	−0.101	0.015	7.29E-11	0.36	−0.101	0.019	7.51E-08	0.45	−0.097	0.034	4.00E-03	0.41
8	rs235770	20	6761764	*BMP2*	T/C	−0.089	0.016	1.57E-08	0.39	−0.088	0.017	1.34E-07	0.33	−0.087	0.050	8.20E-02	0.78